

# Cross-Linked Hyperbranched Arylamine Polymers as Hole-Transporting Materials for Polymer LEDs

Geeta Kheter Paul, Jeremiah Mwaura, Avni A. Argun, Prasad Taranekar, and John R. Reynolds\*

The George and Josephine Butler Polymer Laboratories,  
Department of Chemistry and Center for Macromolecular  
Science and Engineering, University of Florida,  
Gainesville, Florida 32611

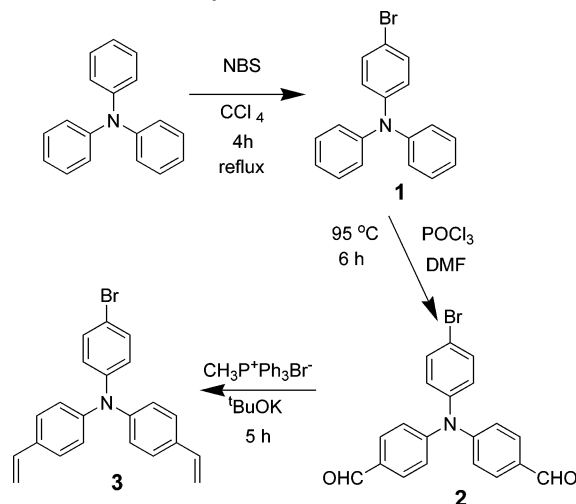
Received April 10, 2006

Revised Manuscript Received September 12, 2006

Polymer light-emitting diodes (PLEDs) have been the subject of intense research over the past 15 years because of their potential use in the display industry.<sup>1–3</sup> Charge transport is an important factor with regard to the performance of these devices. For a PLED to be efficient, balanced charge injection and transport are required, so that the electron and hole combination takes place inside the emissive layer away from the electrodes.<sup>4</sup> To achieve optimum device performance, it is desired that the PLEDs have a suitable hole-injection/hole-transport layer<sup>5</sup> that combines good mechanical properties and thermal stability. Examples of commonly used hole-injection layers (HILs) which possess free charge carriers include p-doped polymers such as PEDOT–PSS,<sup>6</sup> PANI–CSA,<sup>7</sup> and PPy–BDSA.<sup>8</sup> However, because of the acidic nature of these conventional polymers, they have limitations which include corrosion of the ITO surface, while also exhibiting optical absorption in the visible region.<sup>9</sup> One research focus has been directed to the fabrication of fully organic-processable multilayer devices where semiconducting, charge neutral hole-transport layers (HTLs) are the key.<sup>10</sup> Such organic-processable multilayer devices provide a challenge as dissolution of a deposited layer occurs in the solvent of the subsequent layer. One approach to circumvent this problem was to use an organic-soluble precursor PPV, which became insoluble upon thermal treatment.<sup>11</sup> Another way to overcome the solubility problem is by cross-linking of the first layer, which can be achieved by exposure to UV light<sup>12–18</sup> or thermal cross-linking.<sup>18–20</sup>

To date, most polymer HTLs have been linear structures, with little attention paid to 3-dimensional network polymers.<sup>21</sup> Hyperbranched polymers provide a unique entry into network polymers as their branched structures allow unusual physical and chemical properties which include high solubility, low intrinsic viscosity, and a large number of terminal and potentially reactive functional groups.<sup>22</sup> The segments in the hyperbranched polymers possess limited intra- and intermolecular interactions that reduce the possibility of unwanted processes, such as aggregation and interchain exciton formation. Hence, these polymers would lead to organic electronic devices with improved stability and efficiency over those made using general linear polymers. With these objectives in mind, we have designed a triphenylamine-based cross-linkable hyperbranched polymer with extended diamine conjugation. Triphenylamine-based materials are a well-known class of hole-transporting materials and constitute a key feature of many HTLs<sup>23,24</sup> since they tend to form a stable dication. We have chosen the AB<sub>2</sub> monomer 4-bromo-*N,N*-

Scheme 1. Synthesis of Monomer (BVPA)

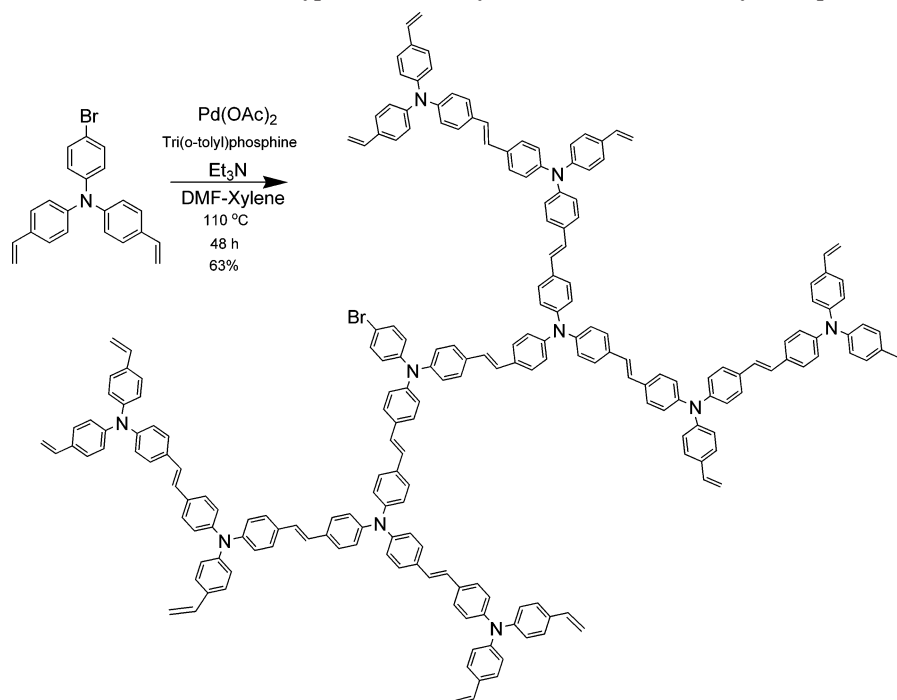


bis(4-vinylphenyl)aniline (BVPA) to generate this hyperbranched polymer and report its synthesis and utility as an HTL here.

BVPA (**3**) was synthesized via the reaction sequence shown in Scheme 1, and the structures were fully characterized by <sup>1</sup>H NMR, <sup>13</sup>C NMR, HR-MS, and elemental analysis (see the Supporting Information for the synthesis and structural characterization results). This AB<sub>2</sub>-type monomer was successfully polymerized via Heck polycondensation outlined in Scheme 2, and the hyperbranched products were purified by repeated reprecipitation from THF solution into methanol to remove the residual metal catalyst and low molecular weight oligomers. The hyperbranched polymer was characterized by <sup>1</sup>H NMR, <sup>13</sup>C NMR, and FT-IR spectroscopy, through which it was specifically inferred that the terminal vinylene groups were stable under the Heck polymerization conditions. The <sup>1</sup>H NMR spectra of the polymers show the presence of the styryl end groups. (see the Supporting Information for the structural characterization results). This hyperbranched polymer had an *M<sub>n</sub>* of 23 500 g/mol and a polydispersity of about 2.0 as measured by GPC using a light scattering detector. Because of the hyperbranched nature of the polymer, and despite the lack of solubilizing side chains typically used with conjugated polymers, HB–BVPA was soluble in common solvents which included THF, chloroform, dichloromethane. The polymer also formed optically transparent and fluorescent films on spin-coating.

The thermal properties of this polymer were studied by DSC and TGA. TGA measurements showed the polymer to be stable up to 350 °C under argon. DSC showed an exothermic transition at 150 °C corresponding to the heat of cross-linking on a first scan with no evident thermal transitions on a repeated scan (see Supporting Information). The polymer was cross-linked by heating under dynamic vacuum for 2 h at 150 °C. The solubility of the cross-linked films was studied by investigating the UV–vis spectra before and after washing with THF, which is an excellent solvent for the non-cross-linked polymer. Cross-linking at 150 °C or above yielded fully insoluble film with no change in the electronic absorption spectra, indicating no reaction of the charge-transporting centers as desired (see Supporting Information). It is expected that the internal and stilbene-like

Scheme 2. Chemical Structure of the Hyperbranched Polymer HB-BVPA with Vinyl Groups at the Periphery



double bonds would be less reactive than the terminal styrene-like groups. Had reaction occurred through the internal double bonds, this would have changed the UV-vis spectrum of the hyperbranched polymer during heating.

The UV-vis absorption and photoluminescence spectra of the polymer were recorded in solution and on thin films. Figure 1 shows that a model compound **5** in chloroform solution absorbs in the UV with a  $\lambda_{\text{max}}$  at 384 nm while the polymer exhibits a red-shifted absorption with  $\lambda_{\text{max}}$  at 410 nm. The solid state and solution absorption spectra of the polymer had similar  $\lambda_{\text{max}}$  (411 nm), indicating the absence of aggregation in the hyperbranched polymers. Because of the hyperbranched nature of the polymer, there is no significant ordering of the

polymer chains either from aggregation or crystallization, and hence the polymer film is in an amorphous state.

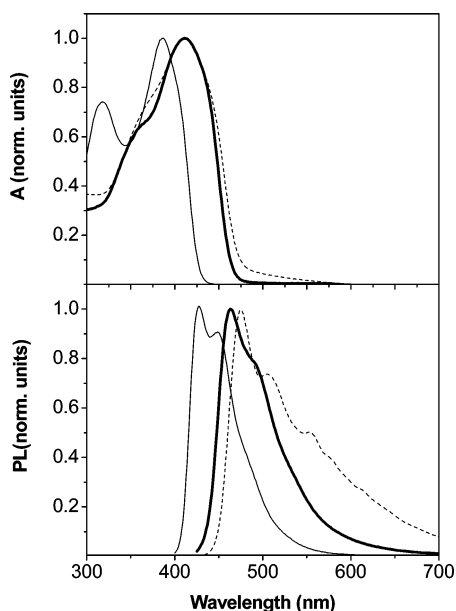
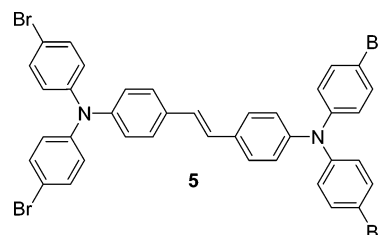


**Figure 1.** UV-vis absorption and photoluminescence spectra of HB-BVPA in solution (—) and solid state (···), along with **5** in solution (---).

Also shown in Figure 1, the model compound in solution displays an emission band at 427 nm while the polymer shows a more red-shifted emission with a  $\lambda_{\text{max,PL}}$  at 462 nm, again indicating an increase in effective conjugation length by polymerization. The polymer film emission spectrum shows a  $\lambda_{\text{max,PL}}$  at 475 nm and exhibits two well-defined vibronic bands at 505 and 555 nm. The red-shifted emission (compared to that of solution) and vibronic bands are due to the formation of a conformation with enhanced conjugation.

The HOMO and LUMO energy levels of HB-BVPA were determined using differential pulse voltammetry (DPV) along with UV-vis absorption spectroscopy. The HOMO level was determined from the sharp oxidation onset of the DPV curve. Using  $E(\text{Fc}/\text{Fc}^+) = 4.8$  eV below the vacuum level, the HOMO level was determined to be 5.1 eV for both the non-cross-linked and cross-linked HB-BVPA. The optical band gap value of 2.6 eV, obtained from the lower energy onset of the absorption spectra, was then used to calculate the LUMO levels (2.5 eV).

The hole-transporting properties of the hyperbranched polymer before and after cross-linking were investigated by fabricating hole-dominated devices with different polymer thicknesses and fitting the current-voltage curves to the space charge limited current (SCLC) model.<sup>25</sup> Diodes were constructed of ITO/PEDOT-PSS/HB-BVPA/Au where the devices were biased so that the hole injection occurs at the PEDOT-PSS/HB-BVPA interface. Because of the high energy barrier

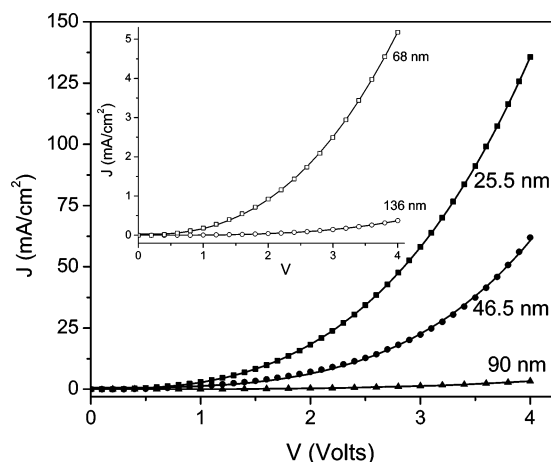


**Figure 2.** Current–voltage characteristics of devices comprising HB–BVPA as the active hole-transporting layers. The actual data points are shown along with the field-dependent mobility fits (solid lines). Inset shows the non-cross-linked polymer  $J$ – $V$  data and their fits.

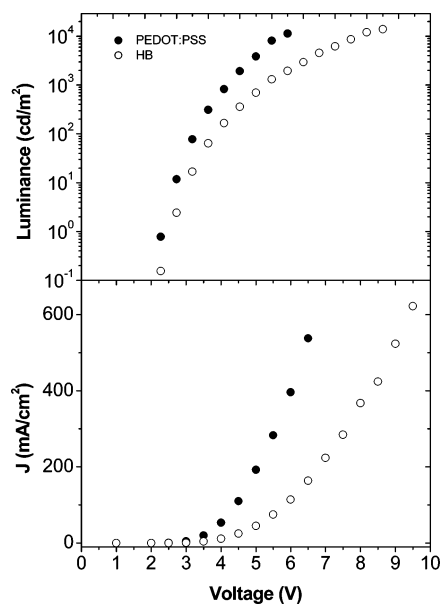
between Au ( $\sim 4.8$  eV) and the LUMO level of the polymer (2.5 eV), the current measured is essentially hole dominated.

Figure 2 shows the current–voltage characteristics of hole-dominated devices comprising as-prepared and thermally cross-linked polymers at different film thicknesses. Thickness was varied to verify that the shapes of  $J$ – $V$  curves were similar, and the current was space charge limited. The  $J$ – $V$  data were fitted using the equation (see Supporting Information)

$$J = \frac{9}{8} \epsilon_r \epsilon_0 \mu(0) e^{\gamma[(V-V')^{1/2}/L]} \frac{(V-V')^2}{L^3} \quad (1)$$

All of the films showed field-dependent hole mobilities as the data points deviate from  $J$ – $V^2$  type behavior at high electric fields. Actual data points are shown along with the solid lines representing the best fit using eq 1. Using the fitting parameters,  $\mu(0)$  is determined to be  $(8.67 \pm 0.69) \times 10^{-8} \text{ cm}^2/(\text{V s})$  with no significant thickness dependence. This value is comparable to the zero-field hole mobility values reported for other hole-transporting polymers such as PPV,<sup>26,27</sup> but lower than regularly packed systems such as regioregular P3HT ( $\sim 10^{-5} \text{ cm}^2/(\text{V s})$ )<sup>28</sup> or molecular TPDs ( $\sim 10^{-3} \text{ cm}^2/(\text{V s})$ ).<sup>29</sup> Data fitting yields  $\gamma$  (field dependence factor) values of  $(2.25 \pm 0.75) \times 10^{-3} (\text{m/V})^{1/2}$ , which is in good agreement with the values reported in the literature for other hole-transport polymers.<sup>26–28,30</sup> The built-in voltage ( $V'$ ), the difference between the work functions of PEDOT–PSS and Au, is obtained from the best fit and varies between 0.15 and 0.30 V. The  $J$ – $V$  data of the non-cross-linked polymers are also fitted using eq 1 and shown in the inset to Figure 2. Best fits of the data (solid lines) yield  $\mu(0)$  and  $\gamma$  values of  $(5.0 \pm 2.12) \times 10^{-8} \text{ cm}^2/(\text{V s})$  and  $(2.06 \pm 1.93) \times 10^{-3} (\text{m/V})^{1/2}$ , respectively. It is important to note that neither thickness difference nor cross-linking seems to have a crucial impact on hole mobility values (see table in Supporting Information).

To demonstrate that cross-linked HB–PVPA serves as an effective HTL, light-emitting devices were fabricated by first spin-casting the hyperbranched polymer (10 mg/mL in chloroform) onto ITO glass substrates with a sheet resistance of  $\sim 10 \text{ } \Omega/\text{sq}$  (Delta Technologies) followed by cross-linking at 150 °C for 2 h under vacuum. The resulting 80 nm thick films were transparent and insoluble. A 50 nm thick MEH–PPV emitting layer was spin-cast on top of the HB–BVPA HTL, followed by Ca (5 nm) and Al (200 nm) layers evaporated in a vacuum



**Figure 3.** Luminance and current density as a function of applied voltage of MEH–PPV PLEDs comprising HB–BVPA (○) and PEDOT–PSS (●) as the HTL.

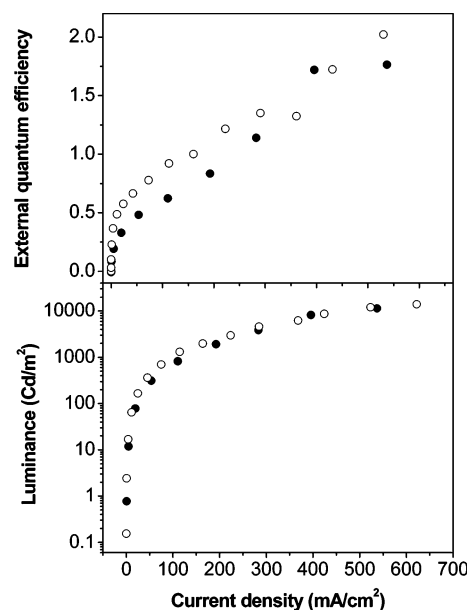


**Figure 4.** Luminance and external quantum efficiency as a function of current density of MEH–PPV PLEDs comprising HB–BVPA (○) and PEDOT–PSS (●) as the HTL.

as the cathode to complete the device. PLEDs with PEDOT–PSS as the HTL were fabricated in parallel for comparison.

Figure 3 shows the device electrical characteristics with the current density and luminance values plotted as a function of drive voltage for both HB–BVPA and PEDOT–PSS devices. As seen from the luminance/voltage results, both devices turn on at  $\sim 3$  V. The electroluminescence (EL) intensifies with increasing voltage at a slightly more gradual rate in the HB–BVPA device compared to the PEDOT–PSS device but still attain quite high luminance values. The  $J$ – $V$  plots for the PLEDs reveal the same trend as the increase in current density with voltage occurs over a broader voltage range in the device with HB–BVPA as the HTL. Comparing the luminance and the external quantum efficiency as a function of current density as shown in Figure 4, the HB–BVPA device performance is essentially identical to the PEDOT–PSS device with both showing a maximum EL emission output of  $\sim 10^4 \text{ cd/m}^2$ . These

initial results indicate that the performance of the cross-linked HB–BVPA as a hole transport layer is comparable to that of PEDOT–PSS. We are currently optimizing the device fabrication in terms of cross-linking and thickness of the HB–BVPA polymer layer. We also believe that the lifetime of the devices fabricated with the benign hyperbranched polymer as the hole-transporting layer will be higher than those with PEDOT–PSS, and studies in this direction are currently underway.

In conclusion, we have prepared a novel AB<sub>2</sub>-type monomer, which upon polymerization yielded a hyperbranched polymer with subsequently polymerizable vinyl groups at the periphery. Thermal polymerization afforded insoluble films, upon which a light-emitting polymer, MEH–PPV, could be spun-cast. The LEDs fabricated using the cross-linked HB–BVPA exhibited comparable or superior performance to devices composed of conventional PEDOT–PSS as HTLs.

**Acknowledgment.** We acknowledge funding of this work by EIC Laboratories (FA 9550-05-C-0147) and the AFOSR (FA955-06-1-0192).

**Supporting Information Available:** Experimental details. This material is available free of charge via the Internet at <http://pubs.acs.org>.

## References and Notes

- Burroughes, J. H.; Bradley, D. D. C.; Brown, A. R.; Marks, R. N.; Mackay, K.; Friend, R. H.; Burn, P. L.; Holmes, A. B. *Nature (London)* **1990**, *347*, 539–541.
- Kraft, A.; Grimsdale, A. C.; Holmes, A. B. *Angew. Chem., Int. Ed.* **1998**, *37*, 403–428.
- Friend, R. H.; Gymer, R. W.; Holmes, A. B.; Burroughes, J. H.; Marks, R. N.; Taliani, C.; Bradley, D. D. C.; Dos Santos, D. A.; Bredas, J. L.; Logdlund, M.; Salaneck, W. R. *Nature (London)* **1999**, *397*, 121–128.
- Strukelj, M.; Papadimitrakopoulos, F.; M.; M. T.; Rothberg, L. J. *Science* **1995**, *267*, 1969–1972.
- Kido, J.; Kimura, M.; Nagai, K. *Science* **1995**, *267*, 1332–1334.
- Cao, Y.; Yu, G.; Zhang, C.; Menon, R.; Heeger, A. J. *Synth. Met.* **1997**, *87*, 171–174.
- Yang, Y.; Heeger, A. J. *Appl. Phys. Lett.* **1994**, *64*, 1245–1247.
- Gao, J.; Heeger, A. J.; Lee, J. Y.; Kim, C. Y. *Synth. Met.* **1996**, *82*, 221–223.
- Jong, M. P. d.; IJzendoorn, L. J. v.; Voigt, M. J. A. d. *Appl. Phys. Lett.* **2000**, *77*, 2255–2257.
- Nalwa, H. S. *Handbook of Advanced Electronic and Photonic Materials and Devices*; Academic: San Diego, CA, 2001; Vol. 10.
- Greenham, N. C.; Moratti, S. C.; Bradley, D. D. C.; Friend, R. H.; Holmes, A. B. *Nature (London)* **1993**, *365*, 628–630.
- Bellmann, E.; Shaheen, S. E.; Thayumanavan, S.; Barlow, S.; Grubbs, R. H.; Marder, S. R.; Kippelen, B.; Peyghambarian, N. *Chem. Mater.* **1998**, *10*, 1668–1676.
- Li, X.-C.; Yong, T.-M.; Grüner, J.; Holmes, A.; Moratti, S.; Cacialli, F.; Friend, R. H. *Synth. Met.* **1997**, *84*, 437–438.
- Domercq, B.; Hreha, R. D.; Zhang, D.; Haldi, A.; Barlow, S.; Marder, S. R.; Kippelen, B. *J. Polym. Sci., Part B: Polym. Phys.* **2003**, *41*, 2726–2732.
- Bacher, A.; Erdelen, C. H.; Paulus, W.; Ringsdorff, H.; Schmidt, H.-W.; Schumacher, P. *Macromolecules* **1999**, *32*, 4551–4557.
- Contoret, A. E. A.; Farrar, S. R.; O'Neill, M.; Nicholls, J. E.; Richards, G. J.; Kelly, S. M.; Hall, A. W. *Chem. Mater.* **2002**, *14*, 1477–1487.
- Bacher, E.; Bayerl, M.; Rudati, P.; Reckefuss, N.; Muller, C. D.; Meerholz, K.; Nuyken, O. *Macromolecules* **2005**, *38*, 1640–1647.
- Sun, H.; Liu, Z.; Hu, Y.; Wang, L.; Ma, D.; Jing, X.; Wang, F. *J. Polym. Sci., Part A: Polym. Chem.* **2004**, *42*, 2124–2129.
- Kläerner, G.; Lee, J. I.; Lee, V. Y.; Chan, E.; Chen, J. P.; Nelson, A.; Markiewicz, D.; Siemens, R.; Scott, J. C.; Miller, R. D. *Chem. Mater.* **1999**, *11*, 1800–1805.
- Liu, S.; Jiang, X.; Ma, H.; Liu, M. S.; Jen, A. K. Y. *Macromolecules* **2000**, *33*, 3514–3517.
- Satoh, N.; Cho, J. S.; Higuchi, M.; Yamamoto, K. *J. Am. Chem. Soc.* **2003**, *125*, 8104–8105.
- Young, H. K. *J. Polym. Sci., Part A: Polym. Chem.* **1998**, *36*, 1685–1698.
- Justin Thomas, K. R.; Lin, J. T.; Tao, Y. T.; Ko, C. W. *Chem. Mater.* **2002**, *14*, 1354–1361.
- U. Bach, K. D. C. H. S. M. G. *Adv. Mater.* **2000**, *12*, 1060–1063.
- Lampert, M. A.; Mark, P. *Current Injection in Solids*; Academic: New York, 1970.
- Blom, P. W. M.; de Jong, M. J. M.; van Munster, M. G. *Phys. Rev. B* **1997**, *55*, R656–R659.
- Bozano, L.; Carter, S. A.; Scott, J. C.; Malliaras, G. G.; Brock, P. J. *Appl. Phys. Lett.* **1999**, *74*, 1132–1134.
- Chiatzun, G.; Kline, R. J.; Michael, D. M.; Ekaterina, N. K.; Jean, M. J. F. *Appl. Phys. Lett.* **2005**, *86*, 122110.
- Strohriegel, P.; Grazulevicius, J. V. *Adv. Mater.* **2002**, *14*, 1439–1452.
- Dmitry, P.; Jenny, N. *J. Appl. Phys.* **2003**, *93*, 341–346.

MA060808P